

1 **An optimised protocol for isolation of RNA through laser capture microdissection of leaf**  
2 **material**

3

4

5 **Lei Hua and Julian M Hibberd**

6

7

8 Department of Plant Sciences, University of Cambridge, Downing Street, Cambridge CB2 3EA,  
9 United Kingdom.

10

11

12 LH - lh556@cam.ac.uk

13 JMH - jmh65@cam.ac.uk

14

15 **Short title:** Improving the isolation of RNA from tissue for laser capture microdissection

16

17 **Keywords:** Laser Capture Microdissection, RNA integrity and yield, rice leaves, mesophyll, bundle  
18 sheath strands

19 **Abstract**

20 Laser Capture Microdissection is a powerful tool that allows thin slices of specific cells types to be  
21 separated from one another. However, the most commonly used protocol, which involves embedding  
22 tissue in paraffin wax, results in severely degraded RNA. Yields from low abundance cell types of  
23 leaves are particularly compromised. We reasoned that the relatively high temperature used for  
24 sample embedding, and aqueous conditions associated with sample preparation prior to  
25 microdissection contribute to RNA degradation. Here we describe an optimized procedure to limit  
26 RNA degradation that is based on the use of low melting point wax as well as modifications to sample  
27 preparation prior to dissection, and isolation of paradermal, rather than transverse sections. Using  
28 this approach high quality RNA suitable for down-stream applications such as quantitative reverse  
29 transcriptase polymerase chain reactions or RNA-sequencing is recovered from microdissected  
30 bundle sheath strands and mesophyll cells of leaf tissue.

## 31 **Introduction**

32 Multicellularity has evolved repeatedly across the tree of life, and is a defining feature of land  
33 plants. Not only does multicellularity solve size and lifespan limitations caused by diffusion and  
34 ageing of individual cells respectively, it also allows increased complexity through the  
35 differentiation of cell types that become specialized for particular functions. Thus, to understand how  
36 a multicellular organism is built and then its structures maintained, analysis of its constituent cell  
37 types is desirable.

38 Various methods have been developed to isolate and study specific cell types in plants. In some  
39 cases, different tissue types can be separated relatively easily. For instance, in some plant species  
40 with C<sub>4</sub> leaf anatomy bundle sheath strands can be separated from the adjoining mesophyll by  
41 differential grinding (Edwards and Black 1971; Kanai and Edwards 1973; Sheen 1995; Covshoff et  
42 al. 2013). However, this is not possible in leaves of species that use the far more prevalent C<sub>3</sub>  
43 pathway, or for tissues in other plant organs, and so more complex approaches have been  
44 developed. Many of these rely on producing transgenic lines in which a cell autonomous reporter  
45 marks a specific cell type such that it can be purified for analysis. This can involve marking cells with  
46 a fluorescent protein to allow fluorescence activated cell sorting (Adrian et al. 2015), or placing an  
47 exogenous tag onto ribosomes (Mustroph et al. 2009; Aubry et al. 2014) or nuclei (Deal and Henikoff  
48 2011; Sijacic et al. 2018) such that they can be immunopurified and mRNAs sequenced and  
49 quantified. The latter approach has been particularly successful in roots where the protoplasting  
50 required is relatively fast (Birnbaum et al. 2003; Brady et al. 2007; Li et al. 2016).

51 However, it is not always possible to generate transgenic plants, or identify a promoter that drives  
52 strong expression in the cell type being studied. In the case of leaves, the process of protoplasting  
53 is known to generate a significant stress response and de-differentiation (Sawers et al. 2007) such  
54 that this approach is compromised if the aim is to better understand photosynthesis. In principle,  
55 laser capture microdissection provides an orthogonal method to these approaches, enabling highly  
56 purified cell populations to be harvested without requiring the generation of transgenic lines (Nelson  
57 et al. 2006). The success of laser capture microdissection largely relies on sample preparation. For  
58 example, thin sections need to be produced, but during fixation, embedding and then sectioning,  
59 good morphological preservation is required for specific cell types to be dissected. At the same time  
60 RNA quality need to be maintained. Freezing and cryosectioning preserve RNA and metabolite  
61 composition, but destroy histological details and so have been used in only limited plant species and  
62 tissue (Kerk et al. 2003; Nakazono et al. 2003). Chemical fixation followed by paraffin embedding is  
63 the most commonly used approach for laser capture microdissection of plant tissue, and so has been  
64 used to study cell types from leaves of rice and maize, as well as tomato fruit, soybean roots and  
65 Arabidopsis flowers (Klink et al. 2005; Wuest et al. 2014; Jiao et al. 2009; Gandotra et al. 2013; Kerk  
66 et al. 2003; Aubry et al. 2014; Aubry et al. 2016). Typically, in these studies non-crosslinking  
67 solutions such as Farmer's fixative or acetone are used to stabilize RNA, and the dehydrated tissue  
68 is then mounted in paraffin wax at ~60°C to allow thin sections to be subjected to microdissection.

69 Although histological details are well preserved using this method, considerable RNA degradation  
70 can take place (Gomez et al. 2009; Roux et al. 2018). We found this to be a particular problem with  
71 low abundance cell types of leaves. To address this issue, we sought to modify existing protocols to  
72 increase RNA yield and integrity during sample processing as well as the laser capture  
73 microdissection procedure itself. By adopting a low-melting point wax, as well as modifying sample  
74 preparation prior to microdissection and isolation of paradermal rather than transverse sections, we  
75 provide a simple and robust method to allow high quality RNA to be obtained from specific cells of  
76 leaves that are not accessible using existing methodologies.

## 77 **Materials and Methods**

### 78 **Plant materials and growth**

79 Seeds of *Arabidopsis thaliana* ecotype Columbia were sown in 1:1 mixture of Levington M3 high  
80 nutrient compost and Sinclair fine Vermiculite soil, vernalized for 3 days and then transferred to a  
81 controlled environment room set at 22°C with a photoperiod of 16h light and 8h dark, a photon flux  
82 density of 200  $\mu\text{mol photons m}^{-2} \text{s}^{-1}$ . Rice (*Oryza sativa* ssp. *indica* IR64) was germinated and grown  
83 in 1:1 mixture of top soil and sand for two weeks in a controlled environment growth room set at  
84 28 °C day 25 °C night, a relative humidity of 60%, a photoperiod of 12h light and 12h dark, and a  
85 photon flux density of 300  $\mu\text{mol m}^{-2} \text{s}^{-1}$ .

86

### 87 **Sample preparation**

88 To evaluate the effect of fixative on RNA integrity, fully expanded leaves of Arabidopsis or rice  
89 were sampled and fixed in ice-cold 100% (v/v) acetone or Farmer's fixative (75% (v/v) ethanol, 25%  
90 (v/v) acetic acid) for 2 hours and 4 hours on ice, respectively, prior to immediate RNA extraction. To  
91 conduct laser capture microdissection rice leaves were cut into 5-8 mm pieces with RNAPrep treated  
92 scissors, and fixed under vacuum for two 10 minutes periods in ice-cold 100% (v/v) acetone and  
93 then left with gentle stirring for 3 hours. Arabidopsis leaves were treated in the same way, but to  
94 maintain tissue structure not subjected to vacuum infiltration. Leaf tissue was then dehydrated  
95 through an ice-cold series of 70%, 85%, 95% and 100% (v/v) ethanol for 1 hour each. Samples were  
96 incubated in 100% (v/v) ethanol overnight at 4°C, prior to being placed in 25%, 50%, 75% and then  
97 100% Steedman's wax at 37°C for 2 hours. This final solution of 100% Steedman's wax was replaced  
98 twice every 2 hours. Tissue was embedded in a 9-cm petri-dish, and after wax had solidified it was  
99 cut into 1 cm<sup>3</sup> blocks and stored in 50 ml falcon tubes with self-indicating silica gel at -80°C.  
100 Steedman's wax was prepared as described (Vitha et al. 2000), 1000 g polyethylene glycol 400  
101 distearate and 111 g 1-hexadecanol were melted at 60 °C and mixed thoroughly, prior to being  
102 aliquoted into 50 ml RNase-free Falcon tubes. Tissue embedded in paraffin wax was also processed  
103 on ice, and dehydration and embedding took place in an automated embedding machine that moved  
104 samples through a series of 50%, 70%, 95% and 100% (v/v) ethanol, followed by 4 x 1 hour  
105 incubations in 100% (v/v) HistoClear, and 2 x 1 hour incubations in Paraplast plus at 60 °C under  
106 vacuum.

107

### 108 **RNA extraction**

109 RNA extraction from whole tissues was undertaken using the RNeasy Plant Mini Kit (Qiagen),  
110 and from microdissected cells using the PicoPure™ RNA Isolation Kit with on-column DNaseI  
111 treatment. To quantify yields 1.5  $\mu\text{l}$  samples of eluted RNA were denatured in 0.2 ml RNase-free  
112 tubes at 70°C for 2 minutes. and 1  $\mu\text{l}$  was analysed using an Agilent Bioanalyser RNA 6000 Pico  
113 assay. Electropherograms were assessed qualitatively for background signal, and the appearance

114 of cytosolic and chloroplastic ribosomal RNA peaks, and quantitatively using the common metrics of  
115 the 25S to 18S ribosomal RNA ratio, and the RNA Integrity Number (RIN) (Schroeder et al. 2006).

116

### 117 **Sectioning and laser capture microdissection**

118 Paradermal sections were prepared using a microtome. Paraffin embedded sections were placed  
119 onto a dry polyethylene naphthalate (PEN) membrane slide (Arcturus) and then floated on diethyl  
120 pyrocarbonate (DEPC)-treated water at 42°C to expand the sections and ensure they were flat.  
121 Water was then removed and slides dried at 42°C for 20 min. Steedman's wax embedded sections  
122 were similarly expanded on DEPC-treated water at room temperature on a PEN membrane slide,  
123 before the slide was dried using tissue paper at room temperature. Before laser capture  
124 microdissection, paraffin wax was removed by incubating slides in 100% (v/v) HistoClear for 5  
125 minutes, whilst Steedman's wax was removed by incubating slides in 100% (v/v) acetone for 1  
126 minute at room temperature. Laser capture microdissection was performed on an Arcturus Laser  
127 Capture Microdissection system using Capsure macro caps to collect bundle sheath strands and  
128 mesophyll cells.

## 129 **Results and Discussion**

### 130 **RNA integrity is maintained with non-crosslinking fixatives**

131 To limit RNA degradation, tissue fixation needs to be rapid. Compared with cross-linking fixatives,  
132 precipitative fixatives such as acetone and Farmer's fixative have commonly been used for laser  
133 capture microdissection sample preparation because they retain good histological detail as well as  
134 reasonable RNA yields (Kerk et al. 2003). However, to our knowledge, a quantitative analysis of the  
135 effect of these fixatives on RNA integrity has not been reported. We therefore fixed Arabidopsis  
136 leaves using acetone or Farmer's fixative on ice for 2 and 4 hours, extracted RNA and found that  
137 yield and integrity were similar after 2 hours and 4 hours fixation using either fixative (Supplemental  
138 Figure 1). This suggests that RNA was preserved well by each of these precipitative fixatives.  
139 However, it was noticeable that leaf tissue sank more rapidly in acetone than in Farmer's fixative,  
140 suggesting a faster penetration into leaf tissue. We therefore subsequently used acetone for sample  
141 preparation.

142

### 143 **RNA integrity is improved after Steedman's wax infiltration**

144 The most commonly used embedding medium for laser capture microdissection studies of plants  
145 is paraffin wax, presumably due to its ease of handling and good preservation of histological details.  
146 Therefore, initially we embedded rice leaves using paraffin wax and transverse sections were  
147 prepared to isolate mesophyll and bundle sheath strands (Figure 1A&B). However, even when a cap  
148 was fully loaded with tissue, which takes around 2 hours of continuous microdissection, very low  
149 quantities of RNA were obtained from bundle sheath strands (Figure 1E). We therefore tested  
150 whether sampling from paradermal sections (Figure 1C&D) improved yields. About ten paradermal  
151 sections could be prepared from one leaf, and in approximately one hour, nearly all of the bundle  
152 sheath strands in these sections could be dissected. This yielded significantly greater amounts of  
153 RNA (Figure 1E). Thus, paradermal sectioning resulted in more tissue being captured per slide  
154 (Figure 1A and 1C), was about twice as quick, and so reduces the risk of RNA degradation. However,  
155 consistent with reports on other tissues (Roux et al. 2018), we also found that RNA quality from  
156 paraffin embedded tissue was low. Since the fixation process itself appeared not to have a  
157 deleterious effect on RNA quality (Supplemental Figure 1), we reasoned that losses in RNA integrity  
158 were caused by fragmentation occurring at the relatively high temperatures associated with  
159 infiltration of paraffin wax. We therefore identified Steedman's wax as an alternative, low-melting  
160 point embedding medium, which has been used in immuno-localization experiments in animals, as  
161 well as laser capture microdissection studies of roots, nodules and embryos (Steedman 1957; Vitha  
162 et al. 2000; Gomez et al. 2009; Thiel et al. 2011; Limpens et al. 2013, Roux et al. 2014).

163 To test the applicability of Steedman's wax for leaf tissue, it was used to embed Arabidopsis and  
164 rice leaves, RNA was extracted from whole microtome sections (without mounting on slides) and the  
165 yield and integrity compared with that recovered from equivalent paraffin-embedded sections. RNA  
166 isolated from tissue in Steedman's wax showed less elevated baselines and clearer peaks

167 representing the cytosolic and chloroplastic ribosomal RNAs (Figure 2A-D). Both the RNA Integrity  
168 Number (RIN) and ribosomal 28S:18S RNA ratio were statistically significantly higher when  
169 Steedman's wax was used to embed Arabidopsis leaves (Figure 2E&F). Although the RIN values  
170 from rice leaves were not increased significantly, it was noticeable that the ribosomal RNA peaks  
171 were more defined, and that the ratio of the cytosolic ribosomal 25S to 18S RNAs was significantly  
172 higher when Steedman's embedding medium was used (Figure 2E&F). Taken together, these  
173 findings indicate that RNA recovered from leaves embedded in Steedman's wax was of higher quality  
174 than that isolated after embedding in paraffin wax. Whilst we are not able rule out other effects, the  
175 simplest explanation is that the lower temperature used during infiltration of Steedman's wax leads  
176 to less RNA damage.

177 To determine whether the duration of infiltration in Steedman's wax affects RNA quality, we  
178 extracted RNA from rice leaf tissue after 1 hour, 3 hours, or 6 hours of infiltration in Steedman's wax.  
179 Both the RIN value and ribosomal 28S to 18S RNA ratio remained essentially unchanged over this  
180 time-course, suggesting that in species that require longer infiltrations for good sectioning, extending  
181 the infiltration time in wax could be used without compromising RNA quality (Supplemental Figure  
182 2).

#### 183 184 **A procedure to minimize RNA degradation during slide preparation**

185 Subsequent to wax embedding, but prior to laser capture microdissection, there are further  
186 opportunities for RNA to be degraded. For example, during slide preparation, sections are typically  
187 expanded by floating on warm RNase-free water at 42°C to ensure they lie flat on the microscope  
188 slides. Water is then removed and samples dried at 42°C for 20-30 minutes. Consistent with RNA  
189 degradation during this process, after slide preparation from paraffin-embedded rice tissue the  
190 cytosolic and chloroplastic ribosomal RNA peaks were less defined, yields were lower, and the 28S  
191 to 18S ribosomal RNA ratio was lower compared with to that isolated from freshly-cut sections  
192 (Figure 3A-D). In contrast, after slide preparation using Steedman's wax for embedding, the cytosolic  
193 and chloroplastic ribosomal RNA peaks were clearly defined, and the 28S to 18S ribosomal RNA  
194 ratio was maintained (Figure 3E-3H). We also found that sections embedded in Steedman's  
195 expanded immediately on water at room temperature (20°C), and that the water could be removed  
196 rapidly by absorption onto soft tissue paper. Adhesion of thin sections to the slide was enhanced by  
197 providing gentle pressure with dry tissue paper (Supplemental Figure 3). This rapid process avoids  
198 the prolonged exposure of sections to higher temperatures and so preserves RNA integrity during  
199 slide preparation. Examination of tissue integrity using light microscopy after embedding in  
200 Steedman's wax showed that histological details were as good as those seen after embedding in  
201 paraffin wax (Supplemental Figure 4).

202  
203  
204



## 205 **High quality RNA can be obtained after laser capture microdissection**

206 To assess the combined impact of the modifications documented above on the final RNA quality  
207 obtained from laser capture microdissection, we compared RNA quality from microdissected tissues  
208 embedded in either paraffin or Steedman's wax. For this purpose, bundle sheath strands and  
209 mesophyll cell sections were captured from both Arabidopsis and rice leaf tissues. RNA isolated by  
210 laser capture microdissection from paraffin embedded sections of either species showed either no  
211 clear, or compromised ribosomal RNA peaks (Figure 4A-D). This was particularly noticeable for the  
212 bundle sheath strands. Moreover, the baseline was high (Figure 4A-D) indicating that the RNA was  
213 severely degraded, and quantitation confirmed these qualitative assessments (Figure 4I-L). In  
214 contrast, RNA isolated from either Arabidopsis or rice tissue embedded in Steedman's wax showed  
215 less elevated baselines, more defined ribosomal RNA peaks (Figure 4E-H), and higher RIN values  
216 and 28S to 18S ribosomal RNA ratios (Figure 4I-L).

217 With the advances and reduced cost of next-generation sequencing, RNA-SEQ has become a  
218 common tool for profiling transcript abundance. However, a high quality RNA input is important for  
219 reliable and reproducible results. For example, it has been reported that RNA degradation can have  
220 a broad effect on quality of RNA-SEQ data, including 3' bias in read coverage, quantitation of  
221 transcript abundance, increased variation between replicates, and reductions in library complexity  
222 (Chen et al. 2014, Feng et al. 2015, Gallego et al. 2014). Indeed, Gallego et al. (2014) found that  
223 RIN values are a robust indicator for RNA degradation, and that RNA-SEQ data from RNA with RIN  
224 values >5 show better correlation with intact RNA. For cell specific profiling of gene expression using  
225 laser capture microdissection, the RIN value of microdissected RNA was rarely >5 when paraffin  
226 wax was used during sample preparation. In contrast, our optimised sample preparation method  
227 using low-melting temperature wax, led to most RNA isolated after microdissection having RIN  
228 values >5. We therefore conclude that these simple modifications allow tissue to be prepared such  
229 that different cell types in the leaf can still be identified, and that the quality of the RNA available for  
230 sampling is improved. We anticipate that this approach will greatly facilitate the analysis of gene  
231 expression in specific cell types of leaves.

232

233

## 234 **Acknowledgments**

235 The work was supported by a C<sub>4</sub> Rice project grant from The Bill and Melinda Gates Foundation to  
236 the University of Oxford (2015-2019).

237

## 238 **Conflict of interest**

239 The authors declare no conflict of interest associated with the work described in this manuscript.

240

241

242

243 **Author contribution**

244 Conceptualization, Lei Hua and Julian M Hibberd; Data curation, Lei Hua and Julian M Hibberd;  
245 Formal analysis, Lei Hua; Funding acquisition, Julian M Hibberd; Investigation, Lei  
246 Hua; Methodology, Lei Hua; Project administration, Julian M Hibberd; Supervision, Julian M  
247 Hibberd; Writing – original draft, Lei Hua; Writing – review & editing, Lei Hua and Julian M Hibberd.

248 **References**

- 249 Adrian, J., Chang, J., Ballenger, C. E., Bargmann, B. O. R., Alassimone, J., Davies, K. A., ...  
250 Bergmann, D. C. (2015). Transcriptome dynamics of the stomatal lineage: birth, amplification  
251 and termination of a self-renewing population. *Developmental Cell*, 33(1), 107.  
252 <https://doi.org/10.1016/J.DEVCEL.2015.01.025>
- 253 Aubry, S., Aresheva, O., Reyna-Llorens, I., Smith-Unna, R. D., Hibberd, J. M., & Genty, B. (2016).  
254 A specific transcriptome signature for guard cells from the C<sub>4</sub> plant *Gynandropsis gynandra*.  
255 *Plant Physiology*, 170(3), 1345-1357.  
256 <https://doi.org/10.1104/PP.15.01203>
- 257 Aubry, S., Kelly, S., Kumpers, B. M. C., Smith-Unna, R. D., & Hibberd, J. M. (2014). Deep  
258 Evolutionary comparison of gene expression identifies parallel recruitment of trans-factors in  
259 two independent origins of C<sub>4</sub> photosynthesis. *PLoS Genetics*, 10(6), e1004365.  
260 <https://doi.org/10.1371/journal.pgen.1004365>
- 261 Aubry, S., Smith-Unna, R. D., Bournsnel, C. M., Kopriva, S., & Hibberd, J. M. (2014). Transcript  
262 residency on ribosomes reveals a key role for the *Arabidopsis thaliana* bundle sheath in sulfur  
263 and glucosinolate metabolism. *The Plant Journal*, 78(4), 659-673.  
264 <https://doi.org/10.1111/tpj.12502>
- 265 Birnbaum, K. et al. (2003). A gene expression map of the *Arabidopsis* root. *Science*, 302(5652),  
266 1956-1960.  
267 <https://doi.org/10.1126/science.1090022>
- 268 Brady, S. M. et al. (2007). A high-resolution root spatiotemporal map reveals dominant expression  
269 patterns. *Science*, 318(5851), 801-806.  
270 <https://doi.org/10.1126/science.1146265>
- 271 Chen, E. A., Souaiaia, T., Herstein, J. S., Evgrafov, O. V., Spitsyna, V. N., Rebolini, D. F., &  
272 Knowles, J. A. (2014). Effect of RNA integrity on uniquely mapped reads in RNA-Seq. *BMC*  
273 *Research Notes*, 7, 753.  
274 <https://doi.org/10.1186/1756-0500-7-753>
- 275 Covshoff, S., Furbank, R. T., Leegood, R. C., & Hibberd, J. M. (2013). Leaf rolling allows  
276 quantification of mRNA abundance in mesophyll cells of sorghum. *Journal of Experimental*  
277 *Botany*, 64(3), 807-813.  
278 <https://doi.org/10.1093/jxb/ers286>
- 279 Deal, R. B., & Henikoff, S. (2011). The INTACT method for cell type-specific gene expression and  
280 chromatin profiling in *Arabidopsis thaliana*. *Nature Protocols*, 6(1), 56-68.  
281 <https://doi.org/10.1038/nprot.2010.175>
- 282 Edwards, G. E., & Black, C. C. (1971). Isolation of mesophyll cells and bundle sheath cells from  
283 *Digitaria sanguinalis* (L.) Scop. leaves and a scanning microscopy study of the internal leaf  
284 cell morphology. *Plant Physiology*, 47(1), 149-156.  
285 <https://doi.org/10.1104/PP.47.1.149>

- 286 Endo, M., Shimizu, H., & Araki, T. (2016). Rapid and simple isolation of vascular, epidermal and  
287 mesophyll cells from plant leaf tissue. *Nature Protocols*, 11(8), 1388-1395.  
288 <https://doi.org/10.1038/nprot.2016.083>
- 289 Endo, M., Shimizu, H., Nohales, M. A., Araki, T., & Kay, S. A. (2014). Tissue-specific clocks in  
290 *Arabidopsis* show asymmetric coupling. *Nature*, 515(7527), 419-422.  
291 <https://doi.org/10.1038/nature13919>
- 292 Feng, H., Zhang, X., & Zhang, C. (2015). mRIN for direct assessment of genome-wide and gene-  
293 specific mRNA integrity from large-scale RNA-sequencing data. *Nature Communications*, 6(1),  
294 7816.  
295 <https://doi.org/10.1038/ncomms8816>
- 296 Gallego Romero, I., Pai, A. A., Tung, J., & Gilad, Y. (2014). RNA-seq: impact of RNA degradation  
297 on transcript quantification. *BMC Biology*, 12(1), 42.  
298 <https://doi.org/10.1186/1741-7007-12-42>
- 299 Gandotra, N., Coughlan, S. J., & Nelson, T. (2013). The *Arabidopsis* leaf provascular cell  
300 transcriptome is enriched in genes with roles in vein patterning. *The Plant Journal*, 74(1), 48-  
301 58.  
302 <https://doi.org/10.1111/tpj.12100>
- 303 Gomez, S. K., Javot, H., Deewatthanawong, P., Torres-Jerez, I., Tang, Y., Blancaflor, E. B., ...  
304 Harrison, M. J. (2009). *Medicago truncatula* and *Glomus intraradices* gene expression in  
305 cortical cells harboring arbuscules in the arbuscular mycorrhizal symbiosis. *BMC Plant*  
306 *Biology*, 9(1), 10.  
307 <https://doi.org/10.1186/1471-2229-9-10>
- 308 Jardinaud MF, Boivin S, Rodde N, Catrice O, Kisiala A, Lepage A, Moreau S, Roux B, Cottret L,  
309 Sallet E, Brault M, Emery RJ, Gouzy J, Frugier F, Gamas P (2016) A laser dissection-RNAseq  
310 analysis highlights the activation of cytokinin pathways by nod factors in the *Medicago*  
311 *truncatula* root epidermis. *Plant Physiology*, 171(3), 2256-2276.  
312 <https://doi.org/10.1104/pp.16.00711>
- 313 Jiao, Y., Lori Tausta, S., Gandotra, N., Sun, N., Liu, T., Clay, N. K., ... Nelson, T. (2009). A  
314 transcriptome atlas of rice cell types uncovers cellular, functional and developmental  
315 hierarchies. *Nature Genetics*, 41(2), 258-263.  
316 <https://doi.org/10.1038/ng.282>
- 317 Kanai, R., & Edwards, G. E. (1973). Separation of mesophyll protoplasts and bundle sheath cells  
318 from maize leaves for photosynthetic studies. *Plant Physiology*, 51(6), 1133-1137.  
319 <https://doi.org/10.1104/PP.51.6.1133>
- 320 Kerk, N. M., Ceserani, T., Tausta, S. L., Sussex, I. M., & Nelson, T. M. (2003). Breakthrough  
321 technologies laser capture microdissection of cells from plant tissues. *Plant Physiology*, 132,  
322 27-35.  
323 <https://doi.org/10.1104/pp.102.018127>

- 324 Klink, V. P., Alkharouf, N., MacDonald, M., & Matthews, B. (2005). Laser Capture Microdissection  
325 (LCM) and expression analyses of *Glycine max* (soybean) syncytium containing root regions  
326 formed by the plant pathogen *Heterodera glycines* (soybean cyst nematode). *Plant Molecular*  
327 *Biology*, 59(6), 965-979.  
328 <https://doi.org/10.1007/s11103-005-2416-7>
- 329 Li, S. et al. (2016). High resolution expression map of the Arabidopsis root reveals alternative  
330 splicing and lincRNA regulation, *Dev Cell*, 39(4), 508-522.  
331 <https://doi.org/10.1016/j.devcel.2016.10.012>
- 332 Limpens E, Moling S, Hooiveld G, Pereira PA, Bisseling T, Becker JD, Küster H. (2013). Cell and  
333 tissue-specific transcriptome analyses of *Medicago truncatula* root nodules. *PLoS One*, 8(5),  
334 e64377.  
335 <https://doi.org/10.1371/journal.pone.0064377>
- 336 Mustroph A, Juntawong P, Bailey-Serres J. (2009). Isolation of plant polysomal mRNA by  
337 differential centrifugation and ribosome immunopurification methods. *Methods in Molecular*  
338 *Biology*, 553,109-126.  
339 [https://doi.org/10.1007/978-1-60327-563-7\\_6](https://doi.org/10.1007/978-1-60327-563-7_6).
- 340 Nakazono, M., Qiu, F., Borsuk, L. A., & Schnable, P. S. (2003). Laser-capture microdissection, a  
341 tool for the global analysis of gene expression in specific plant cell types: identification of  
342 genes expressed differentially in epidermal cells or vascular tissues of maize. *The Plant Cell*,  
343 15, 583-596.  
344 <https://doi.org/10.1105/tpc.008102>
- 345 Nelson, T., Tausta, S.L., Gandotra, N. & Liu, T. (2006). Laser microdissection of plant tissue: what  
346 you see is what you get. *Annual Review of Plant Biology*, 57, 181-201.
- 347 Roux, B., Rodde, N., Jardinaud, M.-F., Timmers, T., Sauviac, L., Cottret, L., ... Gamas, P. (2014).  
348 An integrated analysis of plant and bacterial gene expression in symbiotic root nodules using  
349 laser-capture microdissection coupled to RNA sequencing. *The Plant Journal*, 77(6), 817–837.  
350 <https://doi.org/10.1111/tpj.12442>
- 351 Roux, B., Rodde, N., Moreau, S., Jardinaud, M.-F., & Gamas, P. (2018). Laser capture micro-  
352 dissection coupled to RNA sequencing: A powerful approach applied to the model legume  
353 *Medicago truncatula* in interaction with *Sinorhizobium meliloti*. *Methods in Molecular Biology*,  
354 1830, 191-224.  
355 [https://doi.org/10.1007/978-1-4939-8657-6\\_12](https://doi.org/10.1007/978-1-4939-8657-6_12)
- 356 Satgé, C., Moreau, S., Sallet, E., Lefort, G., Auriac, M.-C., Remblière, C., ... Gamas, P. (2016).  
357 Reprogramming of DNA methylation is critical for nodule development in *Medicago truncatula*.  
358 *Nature Plants*, 2(11), 16166.  
359 <https://doi.org/10.1038/nplants.2016.166>
- 360 Sawers, R. J. et al. (2007). A multi-treatment experimental system to examine photosynthetic  
361 differentiation in the maize leaf. *BMC Genomics*, 8(1), 12.

- 362 [https://doi: 10.1186/1471-2164-8-12](https://doi.org/10.1186/1471-2164-8-12)
- 363 Schroeder, A. et al. (2006). The RIN: an RNA integrity number for assigning integrity values to  
364 RNA measurements, *BMC Molecular Biology*, 7(1), 3.  
365 [https://doi: 10.1186/1471-2199-7-3](https://doi.org/10.1186/1471-2199-7-3).
- 366 Serova, T. A., Tikhonovich, I. A., & Tsyganov, V. E. (2017). Analysis of nodule senescence in pea  
367 (*Pisum sativum* L.) using laser microdissection, real-time PCR, and ACC immunolocalization.  
368 *Journal of Plant Physiology*, 212, 29-44.  
369 <https://doi.org/10.1016/J.JPLPH.2017.01.012>
- 370 Sheen, J. (1995). Methods for Mesophyll and Bundle Sheath Cell Separation. *Methods in Cell*  
371 *Biology*. 49, 305–314.  
372 [https://doi: 10.1016/S0091-679X\(08\)61462-4](https://doi.org/10.1016/S0091-679X(08)61462-4)
- 373 Sijacic, P., Bajic, M., McKinney, E. C., Meagher, R. B., & Deal, R. B. (2018). Changes in chromatin  
374 accessibility between *Arabidopsis* stem cells and mesophyll cells illuminate cell type-specific  
375 transcription factor networks. *The Plant Journal*, 94(2), 215-231.  
376 <https://doi.org/10.1111/tpj.13882>
- 377 Steedman HF (1957) Polyester wax: a new ribboning embedding medium for histology. *Nature*,  
378 179(4574), 1345.
- 379 Thiel, J., Weier, D., & Weschke, W. (2011). Laser-capture microdissection of developing barley  
380 seeds and cDNA array analysis of selected tissues. *Methods in Molecular Biology*, 755, 461-  
381 475.  
382 [https://doi.org/10.1007/978-1-61779-163-5\\_39](https://doi.org/10.1007/978-1-61779-163-5_39)
- 383 Vitha, S; Baluška, F; Volkmann, D; Barlow, PW. (2000). Steedman's wax for F-actin visualization.  
384 Actin: a dynamic framework for multiple plant cell functions. ed. / F.Baluška; P.W.Barlow;  
385 C.J.Staiger; D.Volkmann. Kluwer Academic Publishers, 2000. p. 619 - 636.  
386 [https://doi: 10.1007/978-94-015-9460-8\\_35](https://doi.org/10.1007/978-94-015-9460-8_35)
- 387 Wuest, S. E., & Grossniklaus, U. (2014). Laser-assisted microdissection applied to floral tissues.  
388 *Methods in Molecular Biology*, 1110, 329-344.  
389 [https://doi.org/10.1007/978-1-4614-9408-9\\_19](https://doi.org/10.1007/978-1-4614-9408-9_19)



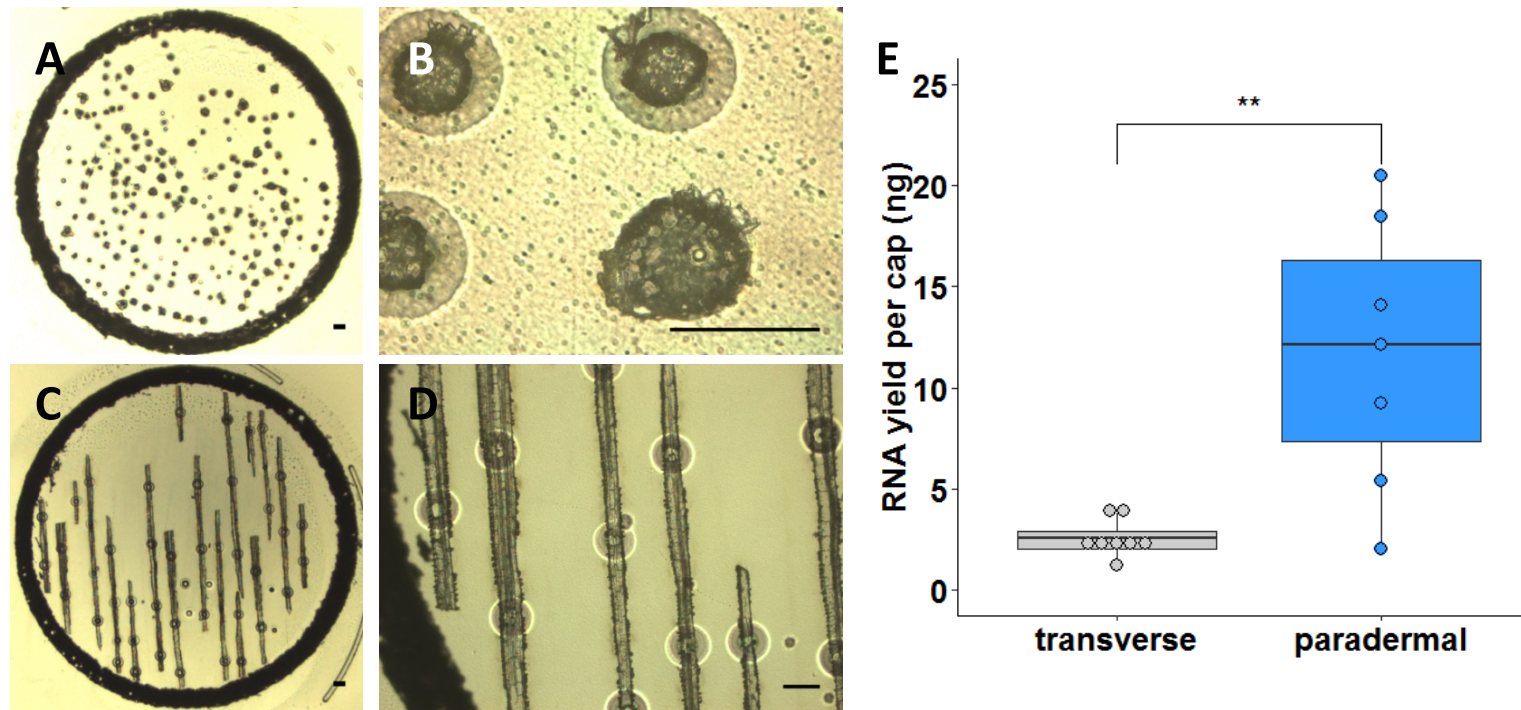


**Figure 1: Isolation of RNA from paradermal sections increases yield from Bundle Sheath Strands (BSS).** Representative images of BSS dissected from transverse (A,B) or paradermal sections (C,D) of rice leaves. A and C show an entire cap used to collect samples after laser capture microdissection. B and D show higher magnification images of individual BSS in transverse (B) or paradermal section (D) respectively. Scale bars represent 100  $\mu$ m. (E) Quantitation of RNA yield after microdissection of BSS tissue from transverse or paradermal sections. Data are derived from 7 or 8 biological replicates, and were subjected to a one tailed t-test, where \*\*  $P < 0.01$ .

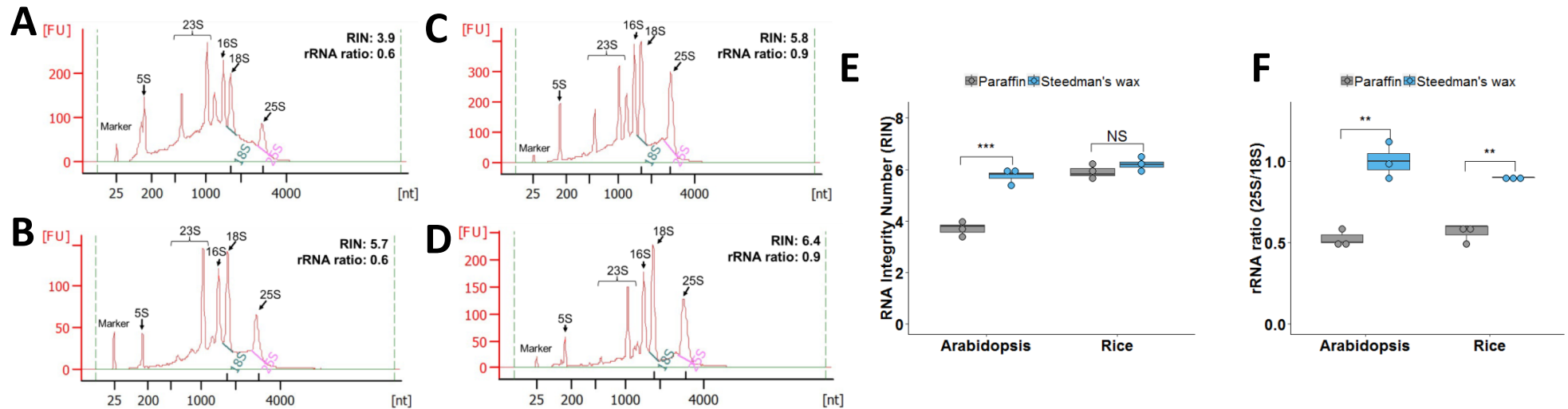


**Figure 2: Steedman's wax improves RNA integrity from sections of Arabidopsis and rice.** Representative RNA profiles of Arabidopsis leaves embedded using paraffin (A) or Steedman's wax (B). Representative RNA profiles of rice leaves embedded using paraffin (C) or Steedman's wax (D). The major ribosomal peaks are annotated. The y-axis shows Fluorescence Units (FU) and the x-axis nucleotide length. Quantitation of RNA Integrity Number (E) and rRNA ratio (F) after embedding in paraffin or Steedman's wax. Both the RNA Integrity Number (RIN) and rRNA ratios were higher when samples were embedded in Steedman's wax. Data were subjected to a one tailed t-test, where NS = Not Statistically different, \*\* P<0.01, \*\*\* P<0.001.



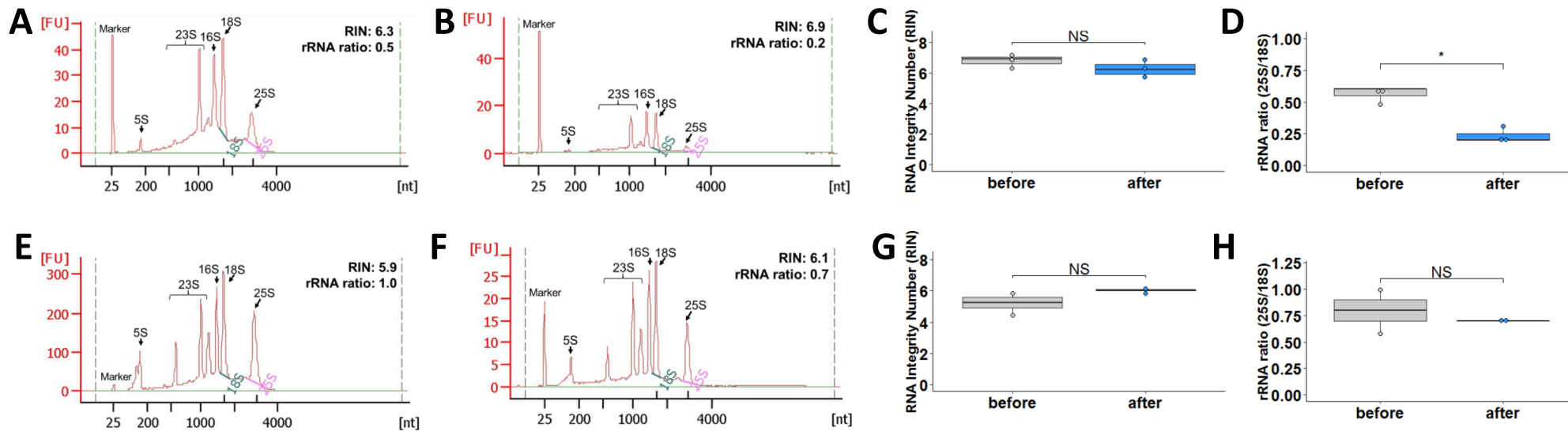


**Figure 3: Limited degradation of RNA from Steedman's wax embedded sections occurs when slide preparation is optimised. (A&B)** Representative RNA profiles of rice sections embedded in paraffin before (A) and after (B) slide preparation. Comparison of RIN (C) and rRNA ratio (D) of paraffin embedded sections before and after slide preparation. **(E&F)** Representative RNA profiles of rice sections embedded in Steedman's wax before (E) and after (F) slide preparation. Comparison of RIN (G) and rRNA ratio (H) of Steedman's wax embedded sections before and after slide preparation. In panels A,B,E&F, the major ribosomal peaks are annotated, the y-axis shows Fluorescence Units (FU) and the x-axis nucleotide length. Data were subjected to a one tailed t-test, where NS = Not Statistically different, \* P<0.05.

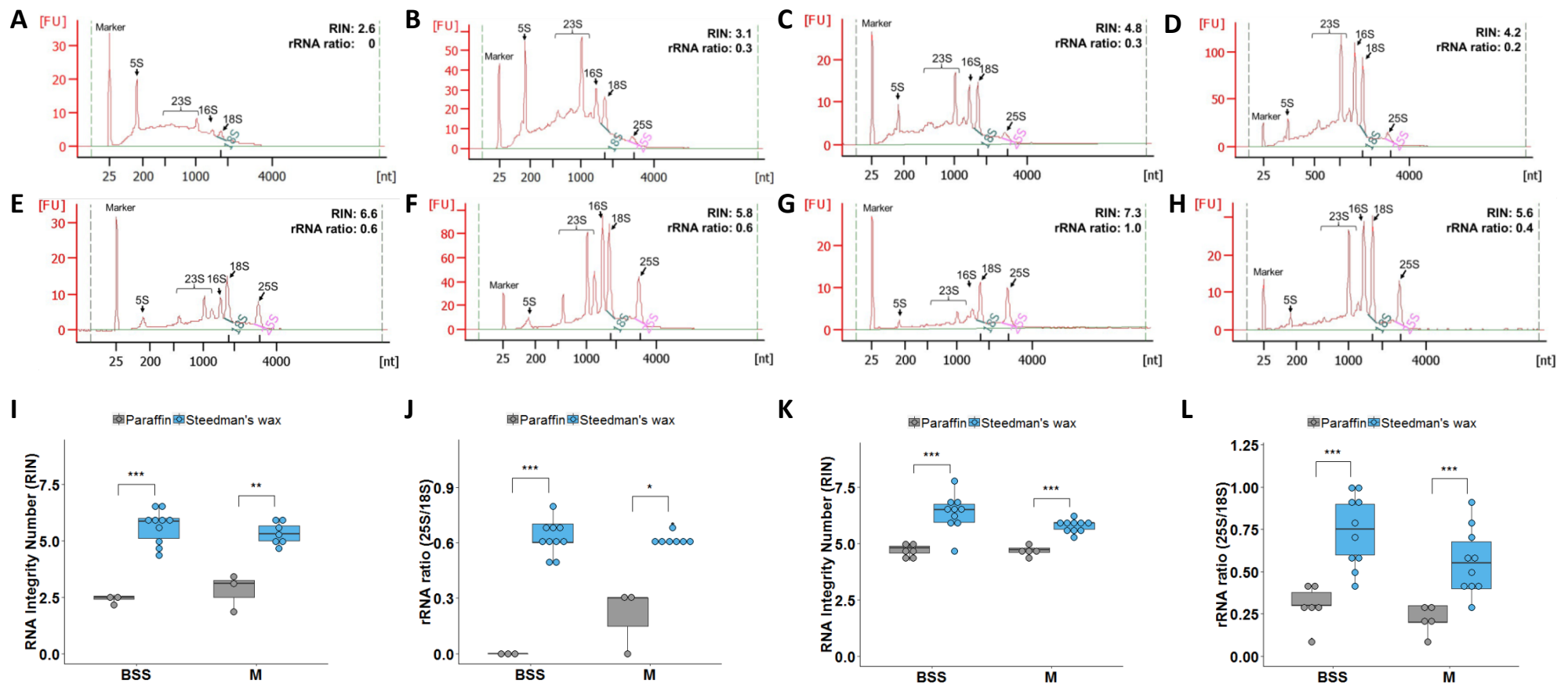


**Figure 4: RNA integrity from Bundle Sheath Strands (BSS) and mesophyll cells is significantly improved when Steedman's wax is used. (A-D)** Representative RNA profiles of microdissected BSS (A, C) or M cells (B, D) from Arabidopsis (A, B) and rice (C, D) embedded in paraffin. (E-H) Representative RNA profiles of microdissected BSS (E, G) or M cells (F, H) from Arabidopsis (E, F) and rice (G, H) embedded in Steedman's wax. The y-axis shows Fluorescence Units (FU) and the x-axis nucleotide length. Note the lower background in Steedman's wax. Comparison of RIN values (I, K) and rRNA ratio (J, L) of RNA extracted from microdissected BSS and M cells from Arabidopsis (I, J) and rice (K, L) embedded using paraffin and Steedman's wax. Data were subjected to a one tailed t-test, where \* P<0.05, \*\* P<0.01, \*\*\* P<0.001.